International Journal of Nanomedicine

Dovepress
Taylor & Francis Group

Open Access Full Text Article

ORIGINAL RESEARCH

# Boosting Radioimmunotherapy by Functionalized Self-Assembled EGCG Nanoparticles Enhances Antitumor Effect for FLASH-RT

Ruiling Xu[1], Xiaowen Han[1], Yunfei Sun[2], Chaofan Ma[2], Shuqing Liao[2], Liu Yang[2], Ruo Tang[2], Zhiyan Zou[1], Xueting Zheng[1], Huiwen Luo[1], Yang Gao[3,4], Xiaozhong He[2], Xiaoan Li[1,5]

[1]NHC Key Laboratory of Nuclear Technology Medical Transformation, Mianyang Central Hospital, School of Medicine, University of Electronic Science and Technology of China, Mianyang, 621000, People's Republic of China; [2]National Key Laboratory for Shock Wave and Detonation Physics, Institute of Fluid Physics, China Academy of Engineering Physics, Mianyang, Sichuan, 621900, People's Republic of China; [3]Institute of Fundamental and Frontier Sciences, University of Electronic Science and Technology of China, Chengdu, Sichuan, 611731, People's Republic of China; [4]Shimmer Center, Tianfu Jiangxi Laboratory, Chengdu, 641419, People's Republic of China; [5]Department of Gastroenterology, Mianyang Central Hospital, School of Medicine, University of Electronic Science and Technology of China, Mianyang, 621000, People's Republic of China

Correspondence: Xiaozhong He, National Key Laboratory for Shock Wave and Detonation Physics, Institute of Fluid Physics, China Academy of Engineering Physics, Mianyang, Sichuan, 621900, People's Republic of China, Email hexiaozhong@caep.cn; Xiaoan Li, NHC Key Laboratory of Nuclear Technology Medical Transformation, Mianyang Central Hospital, School of Medicine, University of Electronic Science and Technology of China, Mianyang, 621000, People's Republic of China, Email lixiaoan@sc-mch.cn



**Background:** With the ability to achieve ideal efficacy while significantly reducing radiation damage to normal tissues, ultra-high dose rate radiotherapy (FLASH-RT) is considered one of the most innovative technologies for cancer treatment in the era of precision medicine. However, compared with conventional radiotherapy (CONV-RT), FLASH-RT has not demonstrated superior efficacy in treating tumors.

**Methods:** We found that the tea polyphenol EGCG could observably promote FLASH-RT X-ray-induced ROS production and DNA damage compared to CONV-RT. A radiosensitizer was further designed by functionalized self-assembled EGCG nanoparticles (named BENPs), aiming to strengthen the anti-tumor effect of FLASH-RT. In vitro experiments such as CCK-8 assay and DNA damage experiment were carried to verify the sensitising effect of BENPs to 4T1 cells. It was further validated in vivo and the molecular mechanism was analyzed using immunofluorescence staining. Biosafety was evaluated by hematoxylin and eosin (H&E) staining and blood routine experiments. Flow cytometry was used to investigate the in vivo immune status of mice triggered by BENPs synergized with FLASH-RT. RNA sequencing assay was employed to estimate the immune response in the spleen of mice.

**Results:** This combined strategy markedly induced apoptosis and necrosis in tumor cells, which availably inhibited the malignant progression of tumors with good biosafety. More than that, BENPs-assisted FLASH-RT facilitated dendritic cell maturation and increased $CD8^+$ Cytotoxic T cells, B lymphocytes, natural killer and memory T cells differentiation, implying the induction of "positive regulation" of the immune microenvironment, with a better immune prognosis. Meanwhile, the activation of immune regulation was confirmed by effectively upregulation of proinflammatory cytokines in the serum.

**Conclusion:** Our study suggests that the potential application of BENPs as a sensitizer for FLASH-RT that brings new inspiration for the future clinical application of FLASH-RT therapy.

**Keywords:** ultra-high dose rate radiotherapy, radiosensitizer, nanoparticles, immune response, tea polyphenol

## Introduction

Radiotherapy (RT) is one of the indispensable means in the treatment of breast cancer. It is commonly used in patients undergoing mastectomy or breast-conserving surgery, as well as in the palliative treatment of patients with advanced breast cancer, which can significantly increase the local control rate and reduce the local and regional lymph node recurrence rate.[1] However, increasing the RT dose causes unnecessary radiation damage to adjacent healthy tissues,[2,3] which not only affects the survival and quality of cancer patients, but also limits the total radiation dose delivered directly

https://doi.org/10.2147/IJN.S571116
Received: 30 October 2025
Accepted: 22 January 2026
Published: 5 February 2026

to the tumor tissue.[4,5] FLASH-Radiotherapy (FLASH-RT) is an innovative radiotherapy technique characterized by ultra-high dose rates with instantaneous, one-time irradiation, which abbreviates course of radiotherapy, increases the tolerance of normal tissues, and provides high efficacy.[6] Studies have shown that FLASH-RT significantly reduced the risk of damage to normal tissues and improved patients' quality of life while ensuring cancer cell killing.[7,8] Unfortunately, tumor cells may repair and adapt to RT-induced changes,[9–11] which can deeply impede the treatment effectiveness of FLASH-RT and lead to tumor recurrence. Fifty-six percent of patients with advanced breast cancer were radiation-resistant, with metastases occurring in the fourteenth month after radiotherapy.[12] Therefore, it is crucial to improve breast cancer resistance to FLASH-RT for better treatment outcomes.

Radiosensitizers are believed to enhance anti-tumor effects by accelerating DNA damage and further free radical production within cancer cells.[13,14] Studies have shown that natural active substances had good biosafety. They had the potential to enhance the radiosensitivity of tumors and might reduce the damage of radiation to normal tissues to a certain extent, thus improving the safety and efficacy of the treatment.[15] It has been shown that epigallocatechin gallate (EGCG), the main active component of catechins in green tea, combined with radiotherapy induced apoptosis in leukaemia cell lines.[16] And EGCG was able to reduce serum vascular endothelial growth factor in patients with breast cancer and activation of metalloproteinases,[17] which significantly weakened tumor malignancy. More than that, the systemic immune response induced by RT is often insufficient to effectively suppress the progression of malignant tumors in clinical practice.[18] Studies have shown that EGCG could enhance the immune function of the body and play a crucial role in the regulation of the innate and adaptive immune system.[19] It can be seen that EGCG has great potential to become a radiosensitizer for clinical application, but there are few studies on EGCG radiosensitization at present.

Interestingly, the effect of FLASH on tumor microenvironment (TME) and tumor-infiltrating immune cells is an under-explored area that deserves further study. The circulating immune cell protection hypothesis widely studied at present points out that, compared with conventional dose-rate radiotherapy, the powerful retention of circulating immune cells by FLASH-RT facilitates the attenuation of the destructive effects on the body's immune system and the repair of damaged tissue cells, thereby reducing the degree of tissue damage.[20] However, recent findings based on different tumor models showed that there was no significant difference in the ability of FLASH-RT and CONV-RT to recruit T lymphocytes,[21–23] which inspired us that in order to enhance the body's immune response, the addition of adjuvants is expected to promote a more pronounced tumor-killing effect of FLASH-RT. Therefore, we devised a strategy of combining EGCG with FLASH-RT to achieve a synergistic anti-tumor effect along with an enhanced immune response.

Unfortunately, like most natural actives, EGCG lacks poor bioavailability,[24] chemical instability,[25] and rapid metabolism, which largely limits its application scenarios.[26] For tumors that are deeply located or adjacent to vital organs, local administration may be risky and infeasible. Intravenous drugs commonly used in clinical practice are distributed systemically through the blood circulation system to reach potential metastatic foci or tumor sites that are difficult to localize on imaging, and are particularly suitable for tumors with indeterminate locations or multiple tumors.[27] Nanoparticles (NPs) offer unique advantages in intravenous administration, especially in drug delivery, targeted therapy and safety. They have been widely studied and applied to improve the efficacy of radiation therapy due to their excellent physicochemical properties, such as good biocompatibility, intrinsic radiosensitizing activity, and enhancement of permeability and retention of tumor tissues (EPR) effects.[28,29]

In view of EGCG assisted FLASH-RT (EGCG@FLASH-RT) was able to effectively induce intracellular ROS generation, apoptosis and DNA damage in tumor cells, furthermore we conducted a simple targeted modification (biotinylated targeting material) of EGCG, which was then self-assembled into nanoparticles (BENPs) and injected intravenously into the body for investigation. In a therapeutic mouse model, in addition to the significant anti-tumor effect under synergistic function, the introduction of BENPs triggered a powerful immune response and induced "positive regulation" of the immune microenvironment (Scheme 1). This novel therapeutic approach is expected to reach a new avenue for the application of FLASH-RT in the field of breast cancer research and provide a promising direction for the future clinical application of FLASH-RT.

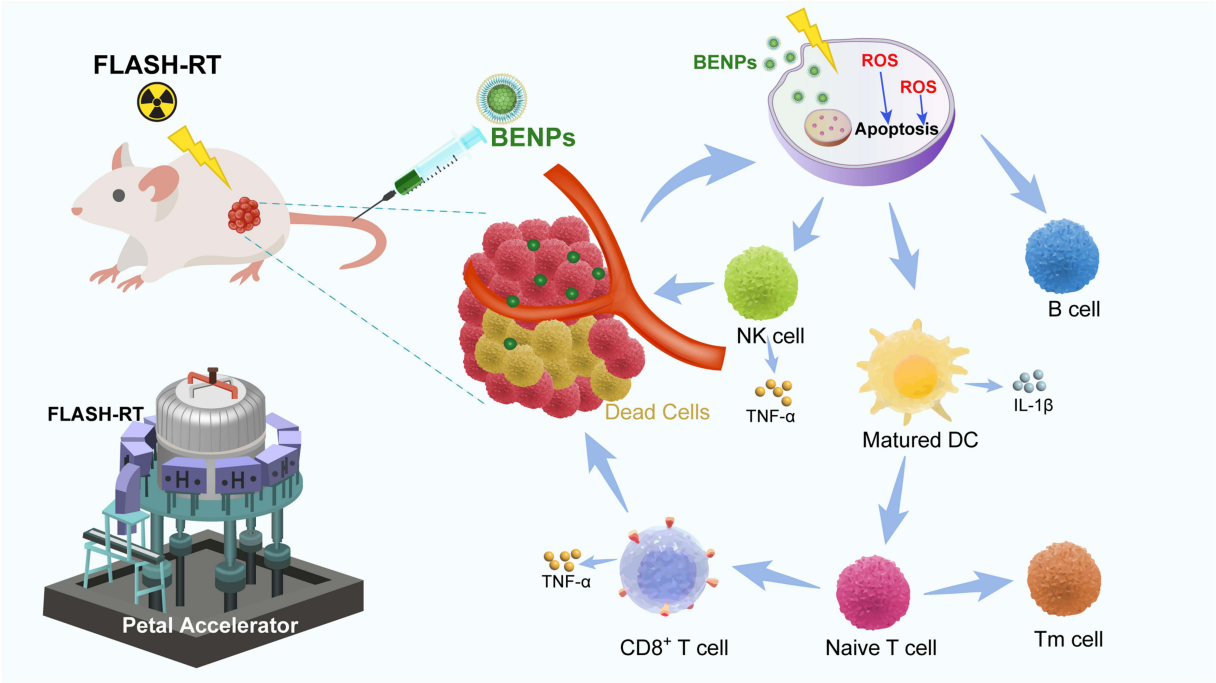


**Scheme 1** After BENPs administration, a large amount of ROS was generated after FLASH-RT, leading to apoptosis of tumor cells, remodeling the immune microenvironment, with a better immune prognosis.

# Materials and Methods

## Materials

EGCG (≥98%) was provided by Shanghai yuanye Bio-Technology Co., Ltd. Biotin-PEG-SH was brought from Guangzhou Tanshtech Co., Ltd. Cell counting kit-8 (CCK-8), penicillin-streptomycin, 1640 medium, PBS, trypsin and fetal bovine serum were brought from Gibco (USA). Gentian violet was provided by Biosharp Technology Co., Ltd. IL-1β/TNF-α cytometric bead array (CBA) kit was purchased from Becton Dickinson (BD, Sunnyvale, CA, USA). Paraformaldehyde was brought from Beyotime Biotechnology Co., Ltd. Annexin V-FITC/7-AAD apoptosis kit, γ-H2AX DNA damage detection kit (mouse mAb/Red) and reactive oxygen species assay kit were obtained from APExBIO Technology LLC. All antibodies used for flow cytometry were brought from BioLegend (CA, USA). All other chemicals and reagents were used as-received without further purification.

## Parameters of FLASH Radiotherapy

In this work, FLASH radiotherapy was carried out via external beam radiation with X-ray from petal accelerator (developed by China Academy of Engineering Physics). Electron energy was 8 MeV. The mean dose rate in the macro-pulse was 94 Gy/s. The source skin distance (SSD) was 16.5 cm for 4T1 cells and 6.45 cm for 4T1-bearing mice. Gafchromic$^{TM}$ EBT3 radiochromic films (Ashland Inc., Covington, Kentucky, USA) were served as absolute dose measurement.

## Cell Cytotoxicity

The 4T1 cells (ATCC no. CRL-2539) were purchased from the American Type Culture Collection (ATCC, Manassas, VA, USA) and maintained in RPMI-1640 medium containing 10% fetal bovine serum. The cell cytotoxicity of EGCG/BENPs was evaluated through CCK-8 experiment. Firstly, 4T1 cells were seeded in 96-well plates at $5\times10^3$ cells/well. After the cells were attached to the wall, the medium was replaced by fresh medium containing different concentrations (10, 20, 30, 40, 60 and 80 μg/mL) of EGCG/BENPs. After 48 h of incubation, the medium was discarded, followed by


https://doi.org/10.2147/IJN.S571116

the addition of CCK-8 dilution to each well, and incubation in the dark for another 4 h. Finally, the absorbance of the reaction solution (450 nm) was measured via a multifunctional microplate reader (Agilent Biotek Synergy Lx). The cell viability (%) was analyzed according to the following formula:

$$\text{Cell viability}(\%) = \frac{OD_b - OD_{blank}}{OD_a - OD_{blank}} \times 100$$

$OD_a$, $OD_b$ and $OD_{blank}$ are the absorbance of control wells without treatment, EGCG/BENPs treated wells and blank wells with the addition of CCK-8 dilution only, respectively.

## Colony Formation Assay

4T1 cells were seeded in 6-well plates ($1\times10^3$ cells/well) and incubated overnight to adherence. Subsequently, the cells were cultured with a fresh medium containing EGCG (30 μg/mL) for 6 h. Then 4T1 cells were exposed to 6 Gy CONV-X-ray (0.1 Gy/s) and FLASH-X-ray (94 Gy/s) radiation. After that, the cells were maintained in fresh culture for 8 days. When clones were formed, cells were fixed using 4% paraformaldehyde for 15 min. Cells were washed twice with PBS and stained with 0.1% crystal violet for 10 min, and three replicates in each group.

## Cell Apoptosis Detection

4T1 cells were collected and seeded in 6-well plates at $2\times10^5$ cells/well and maintained overnight. After the administration of the EGCG treatment, the cells were exposed to 6 Gy CONV-X-ray (0.1 Gy/s) and FLASH-X-ray (94 Gy/s) radiation. Cells were digested by EDTA-free trypsin and resuspended in 1X Binding Buffer. With that, 5 μL Annexin V-FITC and 5 μL 7-AAD were added into the buffer and incubated for 15 min at room temperature. Finally, cell apoptosis was detected by flow cytometry (BD FACSCelesta™ Flow Cytometer).

## Intracellular ROS Detection

4T1 cells were seeded in confocal dishes ($1\times10^5$ cells/well) and cultured for 24 h. After drug treatment for 6 h, the cells were exposed to 6 Gy CONV-X-ray (0.1 Gy/s) and FLASH-X-ray (94 Gy/s) radiation. Subsequently, the DCFH-DA solution (10 μM) was used to stain 4T1 cells for 30 min before removal. In the end, cells were imaged via confocal laser scanning microscope (CLSM, Stellaris 5, Leica, Germany).

## Intracellular DNA Damage Detection

4T1 cells were seeded in confocal dishes at $5\times10^4$ cells/well and cultured overnight to adherence. Cells were cultured with drug solutions for 6 h. Next, 4T1 cells were exposed to 6 Gy CONV-X-ray (0.1 Gy/s) and FLASH-X-ray (94 Gy/s) radiation. After that, cells were fixed with 4% paraformaldehyde and stained by γ-H2AX/DAPI for 30 min. Finally, CLSM was employed to observe the 4T1 cells.

## Preparation and Characterization of Biotin-PEG-EGCG and BENPs

The synthesis of Biotin-PEG-EGCG was fine-tuned based on previous literature reports.[30] More specifically, 18.8 mg EGCG was dissolved in an equal volume of mixed PBS and DMSO solution (20 mL). Then, the mixed solution was added to 5 g/L of Biotin-PEG-SH solution (v/v=1:1). The solution was kept stirred for 7 h (25°C). In the end, an amount of acetic acid was added to the mixture to terminate the reaction (adjust the pH to 4.0). Subsequently, the reaction solution was loaded into a dialysis bag (MWCO = 2000) for purification for 72 h and lyophilized to obtain Biotin-PEG-EGCG and NMR (nuclear magnetic resonance spectrometer, 600 MHz, Bruker Avance 600, Switzerland) was used to characterize the end product. To prepare BENPs, Biotin-PEG-EGCG was dissolved in 4 g/L of chloroform and decompression evaporation was used to get rid of the organic solvent. Then, 4 mL of deionized water was added and incubated with nitrogen for 24 h (45°C). Finally, BENPs was obtained through a 0.45 μm hydrophilic filter. In order to explore the characterization of BENPs, the size distribution and morphology of BENPs were detected by laser particle size analyzer (NanoBrook 90Plus, USA) and HR-TEM (transmission electron microscope, Tecnai G2 F20 S-TWIN, FEI, USA), respectively.

## In vivo Antitumor Efficacy Assay

6–7 weeks female BALB/c mice were injected subcutaneously with 4T1 cells ($5 \times 10^5$/per mouse) to establish a breast tumor model. When tumor sizes reached about 50 $mm^3$, mice were randomly divided into various groups. The groups were injected with equal amounts of PBS and drug solution before X-ray radiation (10 μg/g of drug solution for intratumoral injection, 6 h in advance; 30 μg/g of drug solution for tail intravenous injection, 8 h in advance). The tumors were irradiated by 10 Gy of CONV-X-ray (0.1 Gy/s) and FLASH-X-ray (94 Gy/s). Tumor size (tumor volume = length × $width^2$) and body weight were measured every two days. The mice were euthanized by intraperitoneal injection of a lethal dose of pentobarbital (100 mg/kg, Sigma-Aldrich-P3761) after 10 days. Death usually occurred within 30 minutes. The details for confirming mouse death were as follows: verifying that the mouse exhibited cessation of heartbeat and respiration, remained motionless, displayed dilated pupils, showed no pain response, and demonstrated no reaction when the toe was pressed with a finger or forceps. Satisfaction of these criteria confirmed the animal's death. If vital signs were observed in the mice, the amount of pentobarbital sodium injection should be supplemented as the situation required. Once death was unequivocally confirmed, major organs and tumors (n=4) were collected and fixed with 4% paraformaldehyde and the animal carcasses were stored in the designated freezer. Tissue sections stained with hematoxylin and eosin (H&E). The 4T1 tumor tissue sections were stained with γ-H2AX and TUNEL. Furthermore, blood samples of mice were collected for routine blood analysis and serum IL-1β/TNF-α cytokines were detected by mouse IL-1β/TNF-α cytometric bead array (CBA) kit. All animal procedures have been approved by the guideline for Care and Use of Laboratory Animals Ethical Committee at Mianyang Central Hospital and obtained the necessary approval (S20240204-01).

## In vivo Immune Cell Typing Detection

Immune cells from the spleen in mice were extracted to detect typing. Firstly, spleens were ground up in 3–4 mL PBS and passed through 70 μm screens. Then, cells were collected and lysed for 5 min by erythrocyte lysis solution. Before flow cytometry detection, the collected spleen lymphocytes were stained with FVS-BV605, CD19-PE-CF594, CD11b-Percp-cy5.5, CD45-V500, NK1.1-BV421, CD11c-BV650, F4/80-APC-R700, MHC II-BV786, CD206-PE, CD3-APC-Cy7, CD4-FITC and CD8-APC antibody. In addition, CD45-V500, CD3-APC-Cy7, CD8a-APC, CD62L-PE and CD44-FITC antibody staining was employed to analyze the immune memory effect of T cells (Tm). All data were processed and analyzed by Flowjo-v10.8.1 software, and the relevant gating strategies were displayed in the supplementary figure example (Figure S1).

## Transcriptome Analysis

Transcriptome analysis for the specimens in vivo was implemented by Novogene®. Firstly, RNA was extracted from spleen and its integrity was detected by RNA Nano 6000 Assay Kit. RNA degradation and contamination were monitored to ensure sample quality and the library was subsequently constructed. The size of the inserted fragment and the concentration of the library were detected by Qubit2.0 and Agilent 2100. The library preparations were sequenced on the platform (Illumina Novaseq) to produce 150 bp paired-end reads. Differential expression analysis of two groups/conditions was carried out via the DESeq2R package (1.20.0). Gene expression was performed using FPKM method. *P*-value and false discovery rate (FDR) analysis was adopted to determine significant analysis. Meanwhile, genes with an adjusted *P*-value <=0.05 found by DESeq2 were determined as differentially expressed.

## Statistical Analysis

All data were presented as mean ± standard error of mean. One-way ANOVA was administered to determine statistical significance of experiment results. All statistical analyses were displayed using GraphPad Prism (9.0). $*P < 0.05$, $**P < 0.01$, $***P < 0.001$, $****P < 0.0001$.

# Results and Discussion

## Radiosensitisation of EGCG in vitro

We utilized the petal accelerator to perform ultra-high dose rate radiotherapy with short pulses (94 Gy/s, FLASH-RT) and simulated conventional radiotherapy (0.1 Gy/s, CONV-RT). Firstly, we evaluated the cytotoxic effects of 4T1 cells at

different irradiation doses (6 Gy and 9 Gy) by CCK8 experiments. As shown in Figure 1A, 48 h and 72 h after 4T1 cells were irradiated, we found that both FLASH-RT and CONV-RT had significant cell-killing effects at lower doses (6 Gy) compared with unirradiated cells (Control). Further, we combined EGCG to investigate the synergistic anti-tumor effect with X-ray. EGCG showed certain anti-breast cancer activity and biosafety at the concentration of 30 μg/mL (Figure S2), and we found that 4T1 cells viability was further reduced after EGCG combined with FLASH-RT treatment (Figure 1B). In addition, cell cloning and apoptosis assays were carried out to assess the radiosensitizing ability of EGCG. As shown in Figures 1C and S3, EGCG@FLASH-RT exhibited a significant inhibitory effect on colony formation of 4T1 cells. The results of Annexin V-FITC/7-AAD staining assay showed that CONV-RT caused only about 16.60% apoptosis and FLASH-RT caused approximately 24.74% apoptosis, whereas the apoptosis rate of EGCG@FLASH-RT was as high as 41.80%, which was significantly higher than that of the therapeutic effect of radiotherapy alone (Figure 1D). These results fully indicated that EGCG could effectively enhance the killing effect of FLASH-RT, induce growth inhibition and apoptosis of 4T1 cells, and achieve excellent radiosensitization effect.

It is well known that ROS production and ROS-induced oxidative stress play an important role in tumor progression. The increase of ROS content in cancer cells will aggravate oxidative stress and cause damage to important biological molecules such as DNA, thereby promoting apoptosis or necrosis of cancer cells.[31] Therefore, we subsequently detected the ability of EGCG@FLASH-RT to affect ROS levels and DNA damage in 4T1 cells. In Figure 1E, irradiated cells showed significantly elevated intracellular ROS levels compared to the Control group, with the highest ROS levels in the EGCG@FLASH-RT group. The CLSM images and corresponding 3D reconstructed structures in Figure 1F showed that the EGCG@FLASH-RT group obviously increased intracellular DNA double-strand breaks, suggesting that EGCG had the potential to enhance irradiation-induced cellular damage. Taken together, these results suggested that EGCG prompted ROS overproduction under X-ray irradiation, increased oxidative stress, disrupted redox homeostasis, enhanced radiosensitization, and ultimately led to apoptosis of cancer cells.

## In vivo Radiosensitisation of EGCG@FLASH-RT

Based on the radiotherapy sensitizing properties of EGCG in vitro, we further comprehensively evaluated its role and mechanism of sensitizing FLASH-RT in 4T1-bearing mice. The operation process was shown in Figure 2A, EGCG paratumor administration and FLASH-RT irradiation were given after inoculation of 4T1 cells. According to the dose analysis pictures, a homogeneous dose (10 Gy) was formed at the tumor site, and both CONV-RT and FLASH-RT exhibited consistent light spots, indicating good stability of FLASH (Figure S4). The experimental results in Figure 2B showed that the CONV-RT, FLASH-RT, and EGCG@FLASH-RT groups all inhibited tumor growth to a certain extent compared with the saline group, whereas the EGCG@FLASH-RT group exhibited the most evident tumor inhibition, and the tumor volume was significantly smaller than that of the other treatment-alone groups. Moreover, the tumor weight in the EGCG@FLASH-RT group was significantly lower than that in the other treatment-alone groups, and tumor suppression reached around 85.8% (Figure 2C).

Apart from that, there was no significant change in the body weight of mice receiving treatment in each group (Figure 2D), and the morphology and structure of major organs (heart, liver, spleen, lung, and kidney) in the EGCG@FLASH-RT group were not significantly different from those in the Control group, indicating that there was no significant toxicity effect on the various organs in the mice after administration of the drug (Figure S5A). The blood routine analysis showed a significant reduction of leukocytes in the blood of the CONV-RT group compared with the other groups due to radiation toxicity. The FLASH group and the EGCG@FLASH-RT group were able to restore leukocyte levels to some extent, although the values were lower than those of the control mice, suggesting that FLASH-RT may reduce the adverse effects of radiotherapy on the peripheral blood and is more effective with the addition of EGCG. Apart from that, red blood cells (RBCs), hemoglobin (HGB), and platelets (PLT) in EGCG@FLASH-RT group were not apparently different compared with the Control group (Figure S5B), indicating that EGCG had a high safety as a radiosensitizer in the combined FLASH-RT treatment.

In order to further explore the mechanism of EGCG@FLASH-RT radiosensitization therapy, immunofluorescence analysis of tumor tissues was performed in each treatment group. As shown in the γ-H2AX immunofluorescence sections and the corresponding semi-quantitative results, EGCG@FLASH-RT exhibited the most obvious increase in p-histone

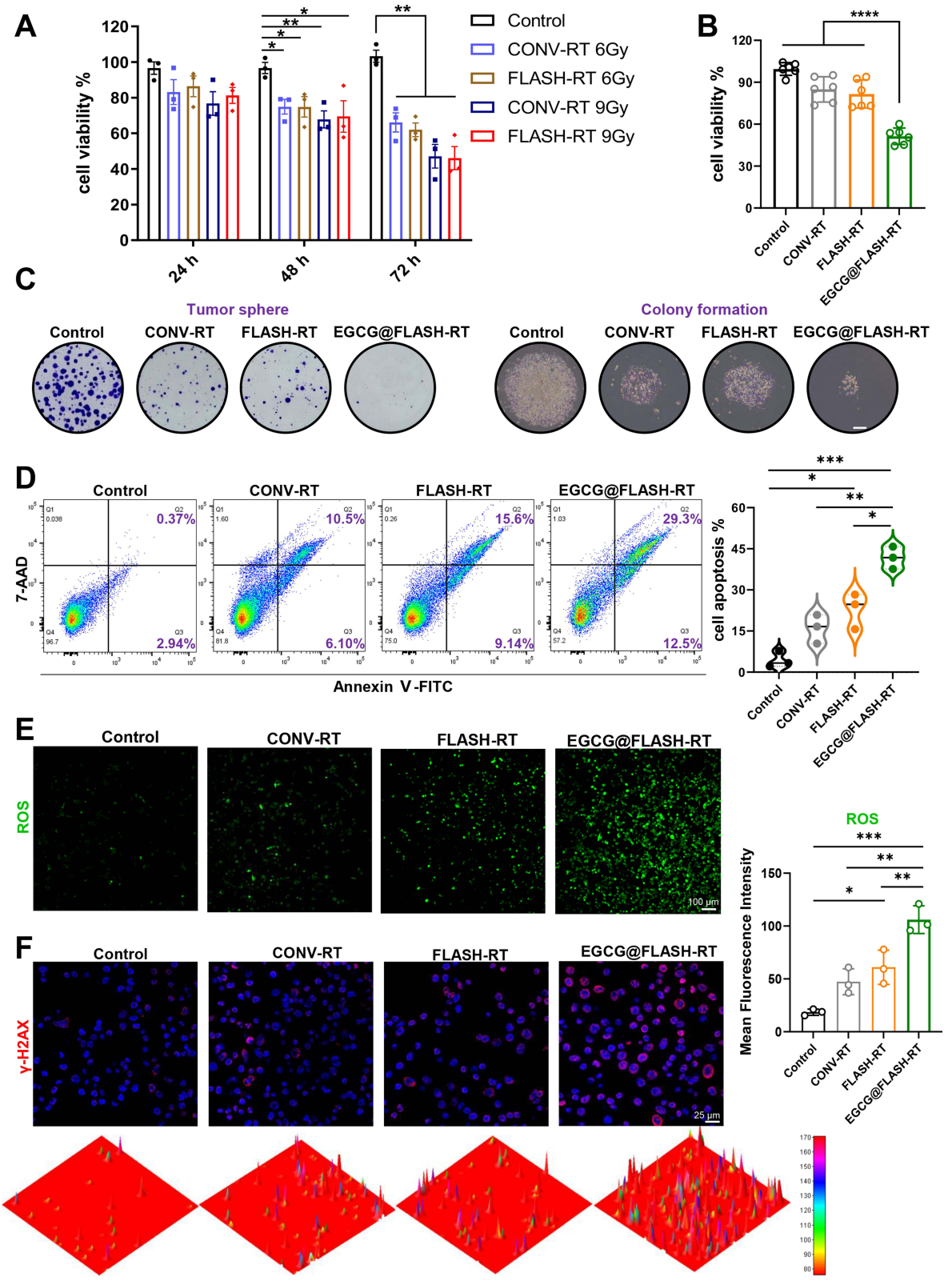


**Figure 1** Evaluation of radiosensitization of EGCG on 4T1 cells in vitro. (**A**) Cytotoxic effects of CONV-RT and FLASH-RT on 4T1 cells. (**B**) Statistical plot of cell viability after treatment of FLASH-RT with EGCG. (**C**) Images of tumor sphere and colony formation after various treatments (scale bar: 250 μm). (**D**) Annexin V-fluorescein isothiocyanate (FITC)/7-Aminoactinomycin D (7-AAD) double staining evaluation of cell apoptosis induced by EGCG@FLASH-RT. (**E**) ROS generation in 4T1 cells after exposure to EGCG@FLASH-RT (scale bar: 100 μm) and corresponding semi-quantitative results. (**F**) CLSM images of γ-H2AX representing DNA double-strand damage under various treatment conditions and 3D reconstruction of γ-H2AX fluorescence by image J (scale bar: 25 μm). All data were presented as the mean ± SD (n≥3). **P* < 0.05, ***P* < 0.01, ****P* < 0.001, *****P* < 0.0001.


https://doi.org/10.2147/IJN.S571116

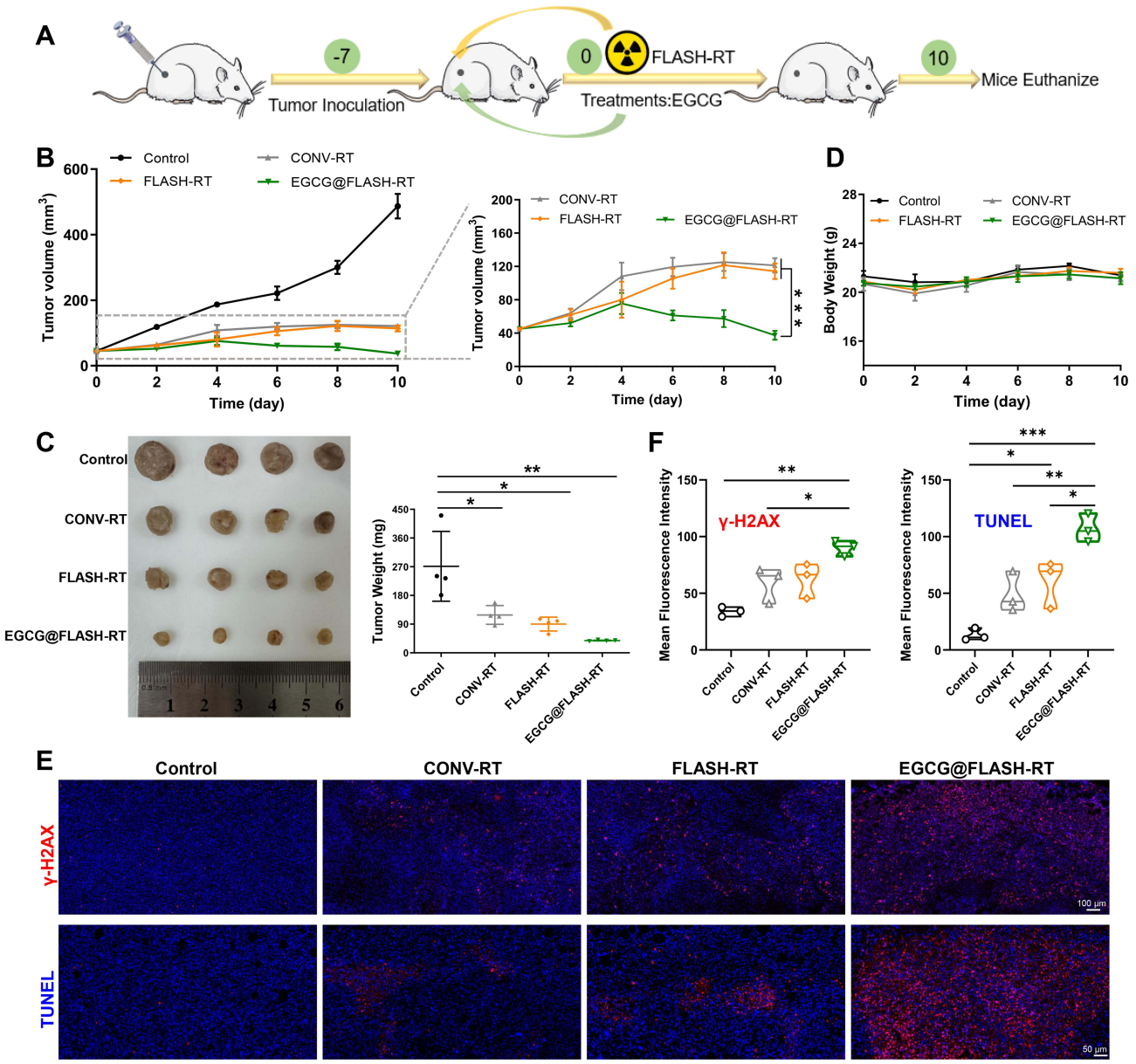


**Figure 2** Antitumor activity of EGCG@FLASH-RT in vivo. (**A**) Schematic illustration of procedure of treatment of EGCG@FLASH-RT. (**B**) Tumor growth curve in different groups within 10 days. (**C**) Images of tumors in each treatment group and corresponding tumor weight. (**D**) Body weight change curve of mice in different groups (n=4 mice per group). (**E**) γ-H2AX and TUNEL immunofluorescence images of tumor sections in different treatment groups (scale bar: 100 μm and 50 μm) and (**F**) corresponding semi-quantitative results. The outcomes were expressed as the mean ± SD (n=3). *$P < 0.05$, **$P < 0.01$, ***$P < 0.001$.

expression, indicating a distinct DNA damage effect (Figure 2E and F). In addition, the red fluorescence of TUNEL was intensified in the EGCG@FLASH-RT group, which caused the most significant tumor cell apoptosis (Figure 2E and F). Overall, these results manifested that EGCG could serve as an excellent radiosensitizer to promote FLASH-RT X-ray-induced DNA damage which in turn enhance tumor apoptosis and necrosis.

## Characterization and Radiosensitisation of BENPs in vitro

Considering the common intravenous drug delivery in clinical practice, nanoparticles have the advantage of targeted aggregation to tumor sites and long circulation in vivo. We further explored by simply modifying EGCG and self-assembling it into nanoparticles. We conducted further exploration after simply modifying EGCG and self-assembling it to form nanoparticles. More specifically, biotin-targeted modification of thiolated polyethylene glycol (Biotin-PEG-SH)


https://doi.org/10.2147/IJN.S571116

was modified onto the EGCG to form Biotin-PEG-EGCG (Figure S6A), and its molecular structures was confirmed by $^{1}$H-NMR (Figure S6B). The blue labeled boxes indicated the characteristic peaks of Biotin and the yellow labeled boxes marked the characteristic peaks of EGCG. Then, Biotin-PEG-EGCG formed nanoparticles (BENPs) by self-assembly under nitrogen incubation, as shown in Figure 3A. Transmission electron microscopy (TEM) images confirmed that the BENPs were spherical (Figure 3B) and the particle size distribution graph showed that the size of BENPs was around 146 nm with good dispersibility (Figure 3C). The Tyndall phenomenon of BENPs could be clearly observed in Figure 3D. In addition, from the release kinetics curve in the Figure S6C, it could be seen that BENPs released slowly in the PBS solution and reached equilibrium after 96 hours. At a concentration of 80 μg/mL, the BENPs significantly inhibited the proliferation of 4T1 cells but exhibited good biocompatibility and were not cytotoxic to normal murine NIH3T3 cells, thus 80 μg/mL was selected as the concentration of BENPs with anti-tumor effects (Figure 3E). To investigate the cellular uptake ability of BENPs, the fluorescent dye Dil was encapsulated by Biotin-PEG-EGCG to form the nanoparticles (Dil-BENPs) used for tracing. After incubation of Dil-BENPs with 4T1 cells for 6 h, fluorescence overlap was observed under CLSM indicating that the nanoparticles were endocytosed into the cell interior (Figure 3F). In addition, immunofluorescence staining of γ-H2AX under CLSM revealed that BENPs visibly enhanced intracellular DNA double-strand breaks, suggesting that the synergistic effect of BENPs with FLASH-RT significantly exacerbated DNA damage (Figure 3G).

## In vivo Radiosensitization of BENPs@FLASH-RT After Trans-Tail Vein Administration

Based on the good sensitization to FLASH after paratumoral injection of EGCG, we further explored the antitumor ability of BENPs-assisted FLASH-RT by using the commonly used intravenous administration method in clinical practice. Consistent with the previous operation except that the mode of administration was changed to tail vein injection (Figure 4A). The dose analysis image showed that a uniform light spot could be formed after irradiation by FLASH (Figure S7). The tumor growth curve (Figure 4B) showed that $EGCG_{i.v.}$@FLASH-RT and BENPs@FLASH-RT group both observably inhibited tumor growth compared with the saline group. In comparison with $EGCG_{i.v.}$@FLASH-RT group, BENPs@FLASH-RT group had smaller tumor showing better tumor inhibition (Figure 4C). As can be seen in Figure S8, it was distinct that the morphological structure of the major organs in the BENPs@FLASH-RT groups mice was not clearly different from that of the control group indicating that there were no apparent toxic effects after trans-tail vein administration. Besides that, there were no abnormalities in the blood routine indicators and stable weight changes (Figure S9) implying that BENPs had a good biosafety. Furthermore, TUNEL and γ-H2AX immunofluorescence sections and the corresponding semi-quantitative results showed that both $EGCG_{i.v.}$@FLASH-RT and BENPs@FLASH-RT groups could promote apoptosis (Figure 4D) and DNA damage (Figure 4E) of tumor cells to a certain extent, and the tumor-killing effect of BENPs@FLASH-RT was more significant.

## In vivo Immune Effects of BENPs@FLASH-RT

Tumor development and progression were closely related to the function of the immune system. We further extracted and analyzed the phenotypes of lymphocytes in the spleens of mice to explore the immune response of BENPs-sensitized FLASH-RT in vivo compared to FLASH-RT. The operation flow chart is shown in Figure 5A, compared with the Control and FLASH-RT group, BENPs@FLASH-RT could signally promote the activation of dendritic cells (DC) in the spleen (Figure 5B). It was noteworthy that the BENPs@FLASH-RT group not only significantly facilitated the maturation of DC but also increased the differentiation of B lymphocytes (Figure 5C), which demonstrated that the combination of BENPs and FLASH-RT was beneficial to strengthen antigen presentation. Moreover, as shown in Figure 5D, BENPs@FLASH-RT group was able to markedly stimulate the differentiation of $CD8^+$ T cells, and the proportion of $CD8^+$ T cells was around 2.3 times that of the Control group, which showed that BENPs@FLASH-RT could intensify the immune response in mice, and the immune response of T cells was significantly biased in the direction of anti-tumor. Memory T (Tm) cells were crucial for maintaining the body's durable immune protection and responding to the prognostic ability of tumor treatment,[32] $CD8^+$ T lymphocytes were further stained to analyze the immune memory response. As the results shown in Figure 5E, the proportion of $CD8^+$ T Tcm (central memory T cells, $CD44^+CD62L^+$) was about 6.76% in the Control group, while the proportion of Tcm in the BENPs@FLASH-RT group was dramatically

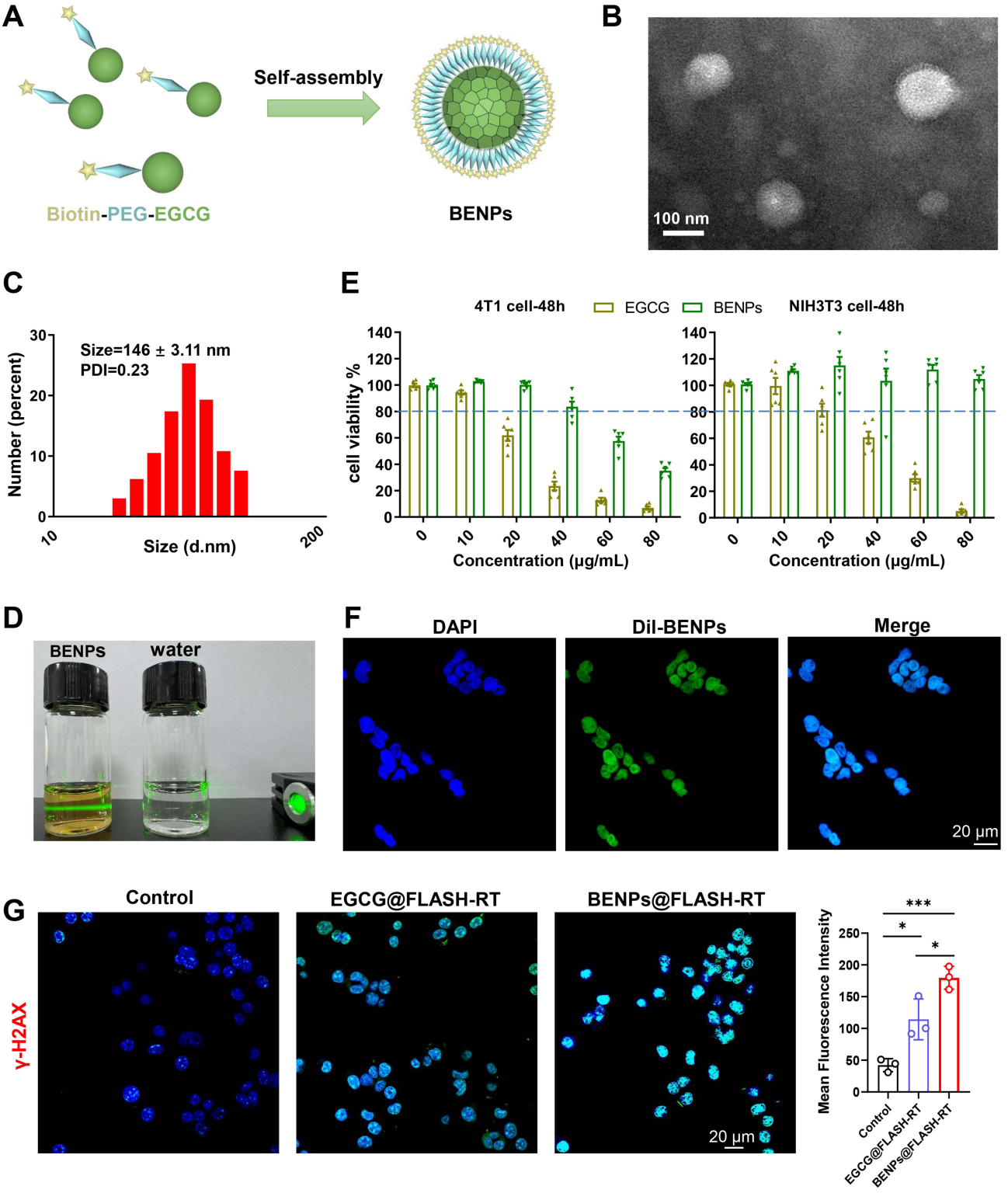


**Figure 3** Preparation and characterization of BENPs. (**A**) Schematic diagram of BENPs fabrication. (**B**) TEM images and (**C**) size distribution of BENPs. (**D**) Tyndall Effect. (**E**) Cell viability of 4T1 and NIH3T3 cells treated with various concentrations of EGCG and BENPs for 48 h (n=6). (**F**) CLSM images for cellular uptake of BENPs (scale bar: 20 μm). (**G**) CLSM images of γ-H2AX representing DNA double-strand damage under various treatment conditions (scale bar: 20 μm, n=3). Significance levels of $^{*}P < 0.05$ and $^{***}P < 0.001$ were applied.


https://doi.org/10.2147/IJN.S571116

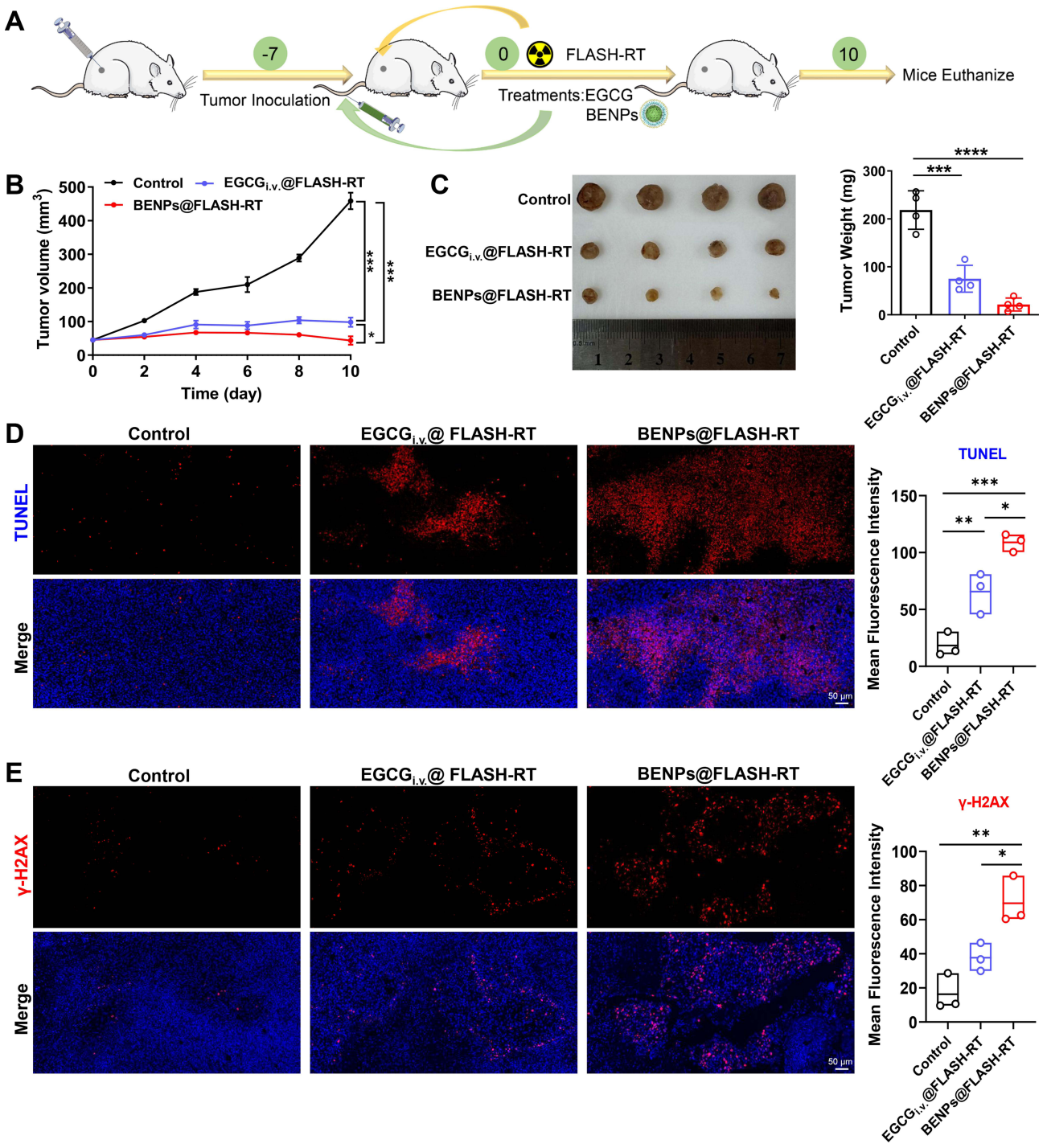


**Figure 4** Antitumor activity of BENPs@FLASH-RT and EGCG$_{i.v.}$@FLASH-RT in vivo after administration via tail vein injection. (**A**) Schematic flow diagram of FLASH-RT of BENPs and EGCG after administration via tail vein injection. (**B**) Tumor volume trends after FLASH-RT. (**C**) Photographs of tumors in various treatment group and corresponding tumor weight (n=4). (**D**) TUNEL and (**E**) γ-H2AX immunofluorescence images of tumor sections in various treatment groups (scale bar: 50 μm) and corresponding semi-quantitative results (n=3). Significance levels of *$P$ < 0.05, **$P$ < 0.01, ***$P$ < 0.001, ****$P$ < 0.0001 were applied.

increased (roughly 23.3%), which was approximately 3.4 times higher than that in the Control group. In addition, the proportion of CD8$^+$ T Tem (effector memory T cells, CD44$^+$CD62L$^-$) in the BENPs@FLASH-RT group had a tendency to increase. The above results indicated that BENPs@FLASH-RT triggered a strong immune memory response with better immune prognostic ability, which was important for inhibiting tumor progression. In addition, the result of blood biochemical test exhibited that the serum expression of IL-1β and TNF-α were at the highest level in the


https://doi.org/10.2147/IJN.S571116

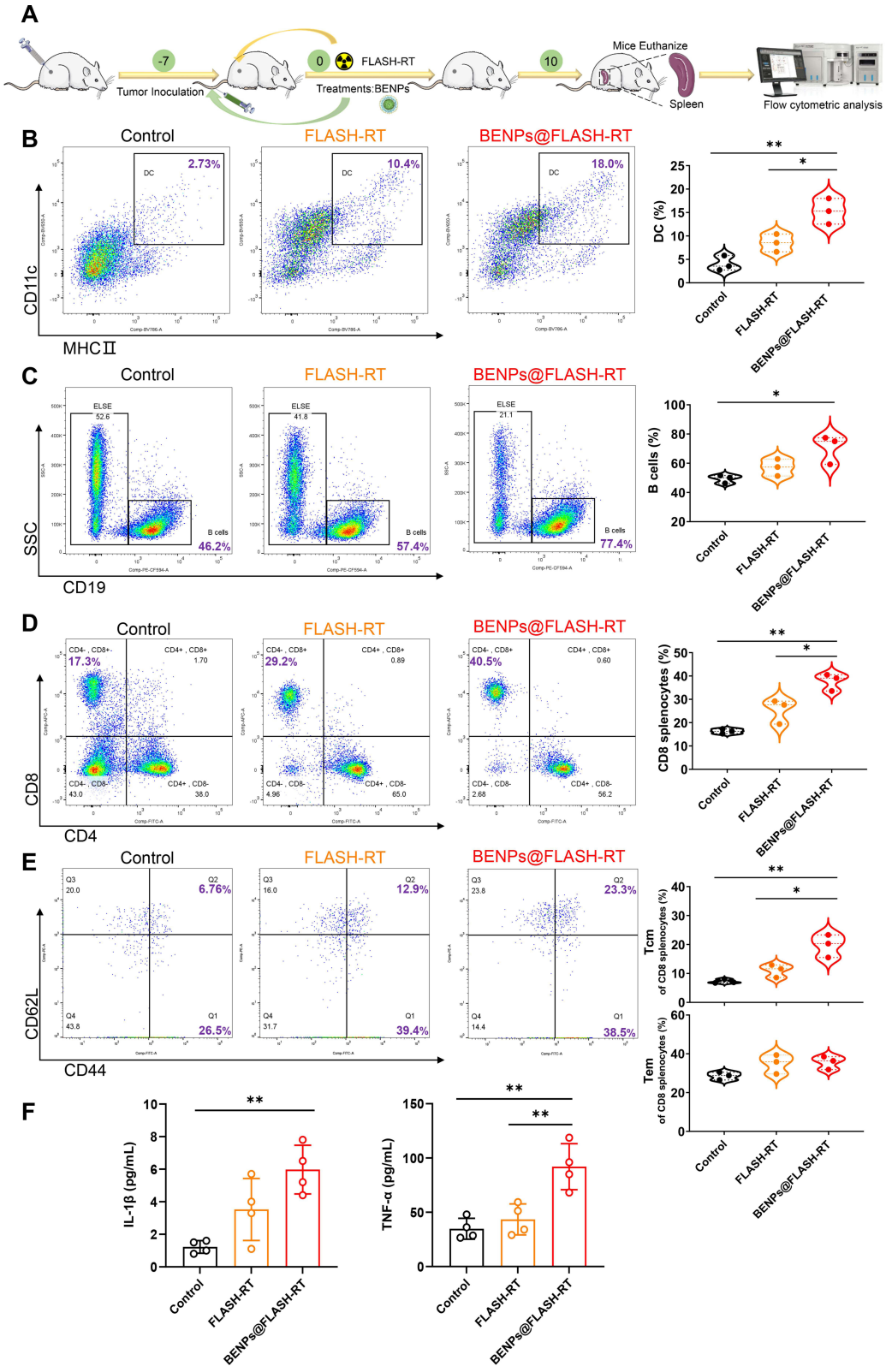


**Figure 5** Evaluation of immune effects after treatment of BENPs@FLASH-RT. (**A**) Schematic illustration of procedure of treatment of BENPs@FLASH-RT. Representative flow cytometry analysis of (**B**) dendritic cell maturation, (**C**) B cells differentiation, (**D**) $CD8^+$ T lymphocytes polarization, (**E**) $CD8^+$ T Tcm and $CD8^+$ T Tem differentiation in the spleen and corresponding quantitative results. (**F**) Analysis of immune factor levels in serum of mice. All data were presented as the mean ± SD (n≥3). $^*P < 0.05$ and $^{**}P < 0.01$.


https://doi.org/10.2147/IJN.S571116

BENPs@FLASH-RT treatment group, demonstrating that a systemic immune response in vivo was induced and the expression of pro-inflammatory factors were increased, which were closely related to tumor growth inhibition (Figure 5F).

## The Immune Response Analysis After BENPs@FLASH-RT Treatment by the Spleen's Transcriptome Sequencing

Spleen is the largest secondary lymphoid organ in the body,[33] which can cause a systemic immune response to attack tumor tissues. It is a momentous part for DC activation,[34] $CD8^+$ Cytotoxic T cells differentiation,[35] and Tcm cell homing.[36] In this study, transcriptomic analysis of spleens after BENPs combined with FLASH-RT treatment was carried out to demonstrate the potential mechanism of BENPs@FLASH-RT-induced immunopotentiation (Figure 6A). According to the GO analysis (Figure 6B), compared with the Control group, the production of molecular mediator of immune response ($P$ value = $3.72\times10^{-15}$), antigen binding ($P$ value = $5.25\times10^{-9}$), B cell mediated immunity ($P$ value = $2.97\times10^{-6}$) and positive regulation of natural killer cell mediated cytotoxicity ($P$ value = $3.87\times10^{-6}$) were notably upregulated indicating that the immune response was activated in the spleen after BENPs@FLASH-RT treatment.

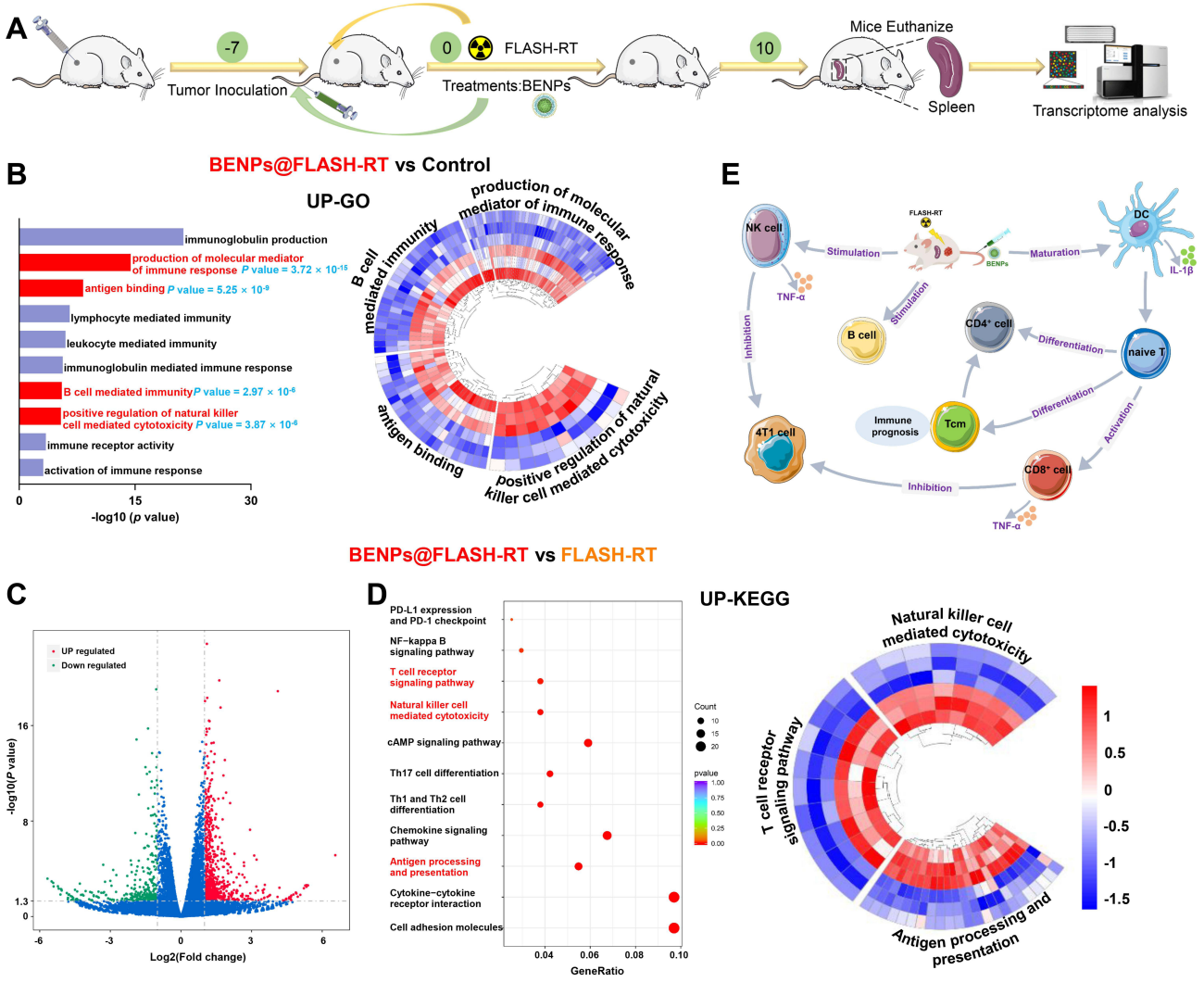


**Figure 6** Transcriptomic analysis of spleen after BENPs@FLASH-RT treatment. (**A**) Schematic illustration of the treatment of BENPs@FLASH-RT for transcriptome analysis. (**B**) The top 10 up-regulated GO terms in BENPs@FLASH-RT vs Control group, and the corresponding heat map of pathways that were highlighted in red. (**C**) Volcano plot of differential gene expression analysis in BENPs@FLASH-RT vs FLASH-RT group. (**D**) Upregulated pathway in enriched KEGG terms in BENPs@FLASH-RT vs FLASH-RT group, and the corresponding heat map of pathways that were highlighted in red. (**E**) Schematic diagram of effect of BENPs@FLASH-RT on the mechanism of immune cell activity in tumor-bearing mice. All data were presented as the mean ± SD (n = 3). *P* values were shown at the top of the graphs.


https://doi.org/10.2147/IJN.S571116

Further, gene expression was further analyzed in BENPs@FLASH-RT vs FLASH-RT to investigate the immune enhancement of sensitizer BENPs. More than 987 genes were significantly regulated in BENPs@FLASH-RT group relative to the FLASH-RT group, which included 664 upregulated genes and 323 downregulated genes ($P$ value < 0.05; Figure 6C). In up-KEGG (Figure 6D), antigen processing and presentation ($P$ value = $1.84\times10^{-6}$) and T cell receptor signaling pathway ($P$ value = 0.00491) were upregulated in BENPs@FLASH-RT group compared to FLASH-RT group, implying that the immune response of T (Th1 and Th2) cell differentiation was activated. In addition, natural killer cell mediated cytotoxicity exhibited apparent upregulation ($P$ value = 0.00141), which might boost the release of relevant cytokines to enhance tumor killing (e.g., noteworthy upregulation of the NF-κB signaling pathway, inflammatory Th17 cell differentiation and cytokine-cytokine receptor interactions). These results indicated that BENPs@FLASH-RT might promote antigen presentation, strengthen natural killer and $CD8^+$ T cells cytotoxicity to activate immune T cell responses (Figure 6E).

## Conclusion

FLASH-RT as an innovative radiotherapy technique is an ideal operation that prominently reduces damage to normal tissues after radiation treatment.[37,38] However, the effect of FLASH-RT in controlling tumor progression is not satisfactory. Here, this study proposed a new strategy of using BENPs as a radiosensitizer to assist FLASH-RT for breast cancer treatment. In vitro and in vivo experiments confirmed that this strategy significantly enhanced tumor cell apoptosis and inhibited the malignant progression of the tumor. Notably, BENPs@FLASH-RT showed promising immunotherapeutic potential, which observably potentiated an in vivo immune response and improved immune prognosis by facilitating dendritic cell maturation and increasing $CD8^+$ Cytotoxic T cell, B lymphocytes, natural killer and memory T cells differentiation. Furthermore, BENPs@FLASH-RT promoted the release of tumor inflammation-associated immunostimulatory factors in mice, activating the immune regulation. Combined with the excellent biosafety, this radiosensitizer BENPs with FLASH-RT has momentous prospects for effectively inhibiting tumor progression, which is expected to advance the field of breast cancer research and bring new inspiration for effective treatment in the clinic.

## Abbreviations

BENPs, functionalized self-assembled EGCG nanoparticles with biotin-modified targeting; CCK-8, cell counting kit-8; CLSM, confocal laser scanning microscope; CBA, cytometric bead array; DC, dendritic cells; EGCG, epigallocatechin gallate; EGCG@FLASH-RT, EGCG assisted FLASH-RT; FLASH-RT, FLASH-Radiotherapy; FDR, false discovery rate; HGB, hemoglobin; PLT, platelets; RT, radiotherapy; ROS, reactive oxygen species; RBCs, red blood cells; SSD, source skin distance; TME, tumor microenvironment; Tm, Memory T; Tcm, central memory T cells; Tem, effector memory T cells; γ-H2AX, phosphorylated H2A histone family member X.

## Funding

This work was sponsored by NHC Key Laboratory of Nuclear Technology Medical Transformation (Mianyang Central Hospital, grant number 2022HYX005, 2024HYX002), Incubation Project of Mianyang Central Hospital (grant number 2023FH011, 2024FH009), Sichuan Science and Technology Program (grant number 2023YFS0470), Mianyang Science and Technology Program (grant number 2023ZYDF073) and Tianfu Jiangxi Laboratory (grant number TFJX-ZD-2024-005).

## Disclosure

The authors declare that they have no known competing financial interests or personal relationships that could have appeared to influence the work reported in this paper.

## References

1. Bartelink H, Maingon P, Poortmans P, et al. Whole-breast irradiation with or without a boost for patients treated with breast-conserving surgery for early breast cancer: 20-year follow-up of a randomised Phase 3 trial. *Lancet Oncol*. 2015;16(1):47–56. doi:10.1016/S1470-2045(14)71156-8

2. You R, Liu YP, Xie YL, et al. Hyperfractionation compared with standard fractionation in intensity-modulated radiotherapy for patients with locally advanced recurrent nasopharyngeal carcinoma: a multicentre, randomised, open-label, phase 3 trial. *Lancet*. 2023;401(10380):917–927. doi:10.1016/S0140-6736(23)00269-6
3. Jiang X, Jiang X, Wu D, et al. A pH-sensitive nanoparticle as reactive oxygen species amplifier to regulate tumor microenvironment and potentiate tumor radiotherapy. *Int J Nanomed*. 2024;19:709–725. doi:10.2147/IJN.S436160
4. Citrin DE. Recent developments in radiotherapy. *N Engl J Med*. 2017;377(11):1065–1075. doi:10.1056/NEJMra1608986
5. Zhang Y, Liu D, Qiao B, et al. Breakthrough of hypoxia limitation by tumor-targeting photothermal therapy-enhanced radiation therapy. *Int J Nanomed*. 2024;19:6499–6513. doi:10.2147/IJN.S450124
6. Ni H, Reitman ZJ, Zou W, et al. FLASH radiation reprograms lipid metabolism and macrophage immunity and sensitizes medulloblastoma to CAR-T cell therapy. *Nat Cancer*. 2025;6:460–473. doi:10.1038/s43018-025-00905-6
7. Weber UA, Scifoni E, Durante M. FLASH radiotherapy with carbon ion beams. *Med Phys*. 2022;49(3):1974–1992. doi:10.1002/mp.15135
8. Vozenin MC, De Fornel P, Petersson K, et al. The advantage of FLASH radiotherapy confirmed in mini-pig and cat-cancer patients. *Clin Cancer Res*. 2019;25(1):35–42. doi:10.1158/1078-0432.CCR-17-3375
9. Suwa T, Kobayashi M, Nam JM, et al. Tumor microenvironment and radioresistance. *Exp Mol Med*. 2021;53(6):1029–1035. doi:10.1038/s12276-021-00640-9
10. de Mey S, Dufait I, De Ridder M. Radioresistance of human cancers: clinical implications of genetic expression signatures. *Front Oncol*. 2021;11:761901. doi:10.3389/fonc.2021.761901
11. Gu J, Mu N, Jia B, et al. Targeting radiation-tolerant persister cells as a strategy for inhibiting radioresistance and recurrence in glioblastoma. *Neuro Oncol*. 2022;24(7):1056–1070. doi:10.1093/neuonc/noab288
12. Yee C, Alayed Y, Drost L, et al. Radiotherapy for patients with unresected locally advanced breast cancer. *Ann Palliat Med*. 2018;7(4):373–384. doi:10.21037/apm.2018.05.13
13. Zhang R, Jia MC, Lv HY, et al. Assembling Au8 clusters on surfaces of bifunctional nanoimmunomodulators for synergistically enhanced low dose radiotherapy of metastatic tumor. *J Nanobiotechnol*. 2024;22:20. doi:10.1186/s12951-023-02279-2
14. Xie J, Gong L, Zhu S, et al. Emerging strategies of nanomaterial-mediated tumor radiosensitization. *Adv Mater*. 2019;31(3):e1802244. doi:10.1002/adma.201802244
15. Zhao X, Luo T, Qiu Y, et al. Mechanisms of traditional Chinese medicine overcoming of radiotherapy resistance in breast cancer. *Front Oncol*. 2024;14:1388750. doi:10.3389/fonc.2024.1388750
16. Baatout S, Derradji H, Jacquet P, et al. Increased radiation sensitivity of an eosinophilic cell line following treatment with epigallocatechin-gallate, resveratrol and curcuma. *Int J Mol Med*. 2005;15(2):337–352.
17. Zhang G, Wang Y, Zhang Y, et al. Anti-cancer activities of tea epigallocatechin-3-gallate in breast cancer patients under radiotherapy. *Curr Mol Med*. 2012;12(2):163–176. doi:10.2174/156652412798889063
18. Li J, Tan C, Yang J, et al. Radiotherapy-immunomodulated nanoplatform triggers both hypoxic and normoxic tumor associated antigens generation for robust abscopal effect and sustained immune memory. *Biomaterials*. 2025;316:123005. doi:10.1016/j.biomaterials.2024.123005
19. Lee H, Jeong JH, Lee T, et al. Identification of (-)-epigallocateshin gallate derivatives promoting innate immune activation via 2',3'-cyclic GMP-AMP-stimulator of interferon genes pathway. *Bioorg Med Chem Lett*. 2023;90:129325. doi:10.1016/j.bmcl.2023.129325
20. Ma Y, Zhang W, Zhao Z, et al. Current views on mechanisms of the FLASH effect in cancer radiotherapy. *Natl Sci Rev*. 2024;11(10):nwae350. doi:10.1093/nsr/nwae350
21. Iturri L, Bertho A, Lamirault C, et al. Proton FLASH radiation therapy and immune infiltration: evaluation in an orthotopic glioma rat model. *Int J Radiat Oncol Biol Phys*. 2023;116(3):655–665. doi:10.1016/j.ijrobp.2022.12.018
22. Almeida A, Godfroid C, Leavitt RJ, et al. Antitumor effect by either FLASH or conventional dose rate irradiation involves equivalent immune responses. *Int J Radiat Oncol Biol Phys*. 2024;118(4):1110–1122. doi:10.1016/j.ijrobp.2023.10.031
23. Zhu H, Xie D, Wang Y, et al. Comparison of intratumor and local immune response between MV X-ray FLASH and conventional radiotherapies. *Clin Transl Radiat Oncol*. 2023;38:138–146. doi:10.1016/j.ctro.2022.11.005
24. Lee MJ, Maliakal P, Chen L, et al. Pharmacokinetics of tea catechins after ingestion of green tea and (-)-epigallocatechin-3-gallate by humans: formation of different metabolites and individual variability. *Cancer Epidemiol Biomarkers*. 2002;Prev 11(10 Pt 1):1025–1032.
25. Krupkova O, Ferguson SJ, Wuertz-Kozak K. Stability of (-)-epigallocatechin gallate and its activity in liquid formulations and delivery systems. *J Nutr Biochem*. 2016;37:1–12. doi:10.1016/j.jnutbio.2016.01.002
26. Zhang L, Zheng Y, Chow MS, et al. Investigation of intestinal absorption and disposition of green tea catechins by caco-2 monolayer model. *Int J Pharm*. 2004;287(1–2):1–12. doi:10.1016/j.ijpharm.2004.08.020
27. Hidalgo M. Pancreatic cancer. *N Engl J Med*. 2010;362(17):1605–1617. doi:10.1056/NEJMra0901557
28. Dou Y, Liu Y, Zhao F, et al. Radiation-responsive scintillating nanotheranostics for reduced hypoxic radioresistance under ROS/NO-mediated tumor microenvironment regulation. *Theranostics*. 2018;8(21):5870–5889. doi:10.7150/thno.27351
29. Bonvalot S, Rutkowski PL, Thariat J, et al. NBTXR3, a first-in-class radioenhancer hafnium oxide nanoparticle, plus radiotherapy versus radiotherapy alone in patients with locally advanced soft-tissue sarcoma (Act.In.Sarc): a multicentre, Phase 2-3, randomised, controlled trial. *Lancet Oncol*. 2019;20(8):1148–1159. doi:10.1016/S1470-2045(19)30326-2
30. Yongvongsoontorn N, Chung JE, Gao SJ, et al. Carrier-enhanced anticancer efficacy of sunitinib-loaded green tea-based micellar nanocomplex beyond tumor-targeted delivery. *ACS Nano*. 2019;13(7):7591–7602. doi:10.1021/acsnano.9b00467
31. Tuli HS, Kaur J, Vashishth K, et al. Molecular mechanisms behind ROS regulation in cancer: a balancing act between augmented tumorigenesis and cell apoptosis. *Arch Toxicol*. 2023;97(1):103–120. doi:10.1007/s00204-022-03421-z
32. Lam N, Lee Y, Farber DL. A guide to adaptive immune memory. *Nat Rev Immunol*. 2024;24(11):810–829. doi:10.1038/s41577-024-01040-6
33. Lewis SM, Williams A, Eisenbarth SC. Structure and function of the immune system in the spleen. *Sci Immunol*. 2019;4(33). doi:10.1126/sciimmunol.aau6085
34. Xiao W, Wang FZ, Gu YZ, et al. PEG400-mediated nanocarriers improve the delivery and therapeutic efficiency of mRNA tumor vaccines. *Chin Chem Lett*. 2024;35:108755. doi:10.1016/j.cclet.2023.108755
35. Im SJ, Hashimoto M, Gerner MY, et al. Defining CD8+ T cells that provide the proliferative burst after PD-1 therapy. *Nature*. 2016;537(7620):417–421. doi:10.1038/nature19330

36. Jung YW, Kim HG, Perry CJ, et al. CCR7 expression alters memory CD8 T-cell homeostasis by regulating occupancy in IL-7- and IL-15-dependent niches. *Proc Natl Acad Sci USA*. 2016;113(29):8278–8283. doi:10.1073/pnas.1602899113
37. Tang R, Yin J, Liu Y, et al. FLASH radiotherapy: a new milestone in the field of cancer radiotherapy. *Cancer Lett*. 2024;587:216651. doi:10.1016/j.canlet.2024.216651
38. Shi X, Yang Y, Zhang W, et al. FLASH X-ray spares intestinal crypts from pyroptosis initiated by cGAS-STING activation upon radioimmunotherapy. *Proc Natl Acad Sci USA*. 2022;119(43):e2208506119. doi:10.1073/pnas.2208506119